The Shape of Word Embeddings: Quantifying Non-Isometry With Topological Data Analysis

Ondřej Draganov
Institute of Science and Technology Austria (ISTA)
Am Campus 1, 3400
Klosterneuburg, Austria
ondrej.draganov@ist.ac.at

Steven Skiena
Dept. of Computer Science
Stony Brook University
Stony Brook, NY 11794-2424 USA
skiena@cs.stonybrook.edu

Abstract

Word embeddings represent language vocabularies as clouds of d-dimensional points. We investigate how information is conveyed by the general shape of these clouds, instead of representing the semantic meaning of each token. Specifically, we use the notion of persistent homology from topological data analysis (TDA) to measure the distances between language pairs from the shape of their unlabeled embeddings. These distances quantify the degree of non-isometry of the embeddings. To distinguish whether these differences are random training errors or capture real information about the languages, we use the computed distance matrices to construct language phylogenetic trees over 81 Indo-European languages. Careful evaluation shows that our reconstructed trees exhibit strong and statistically-significant similarities to the reference.

1 Introduction

Does the *shape* of an unlabeled, monolingual word embedding carry relevant information about the language it represents? Word embeddings are well-established objects of interest in natural language processing, being d-dimensional vector representations that capture the semantics of each vocabulary word. The vocabulary of language L can thus be viewed as a cloud of points, whose geometric and structural properties encode considerable information about the language. In this paper, we demonstrate that, even after disassociated from their bindings to particular words, the "shape" of these point clouds correlates with the history of the languages they represent. We use techniques from *topological data analysis* (TDA), a field studying spatial aspects of data, to quantify this correlation.

How much shapes of word embeddings differ, and for what reasons, is an ongoing debate with important consequences. Many authors assume that the word embeddings of different languages are essentially isometric: meaning they only differ by an orthogonal transformation. Such assumptions are necessary, for example, to construct translators between languages via bilingual lexicon induction (Miceli Barone, 2016; Lample et al., 2018; Zhang et al., 2017). This assumption has been disputed by Søgaard et al. (2018) or Patra et al. (2019). Later Vulić et al. (2020) argued that observed deviations from isometry are largely due to insufficient data or training in construction of embeddings for some languages. In this paper, we demonstrate that these observed non-isometries across languages contain real information and are thus not random training artifacts. We analyze FastText embeddings of 81 Indo-European languages and quantify non-isometry among the 10k most frequent tokens of each language with TDA-based distance matrices. To show that those distances contain real information we construct phylogenetic trees and compare these to a gold-standard reference tree from Ethnologue (Lewis et al., 2024).

The history of language evolution is typically studied by identifying *cognate* word pairs of languages L_1 and L_2, namely homologous word forms inherited from the common ancestor of these languages. Cognates usually share some level of surface-form similarity between them, with language pairs sharing more cognates presumed to be more closely related. The identification of cognate pairs traditionally requires extensive labor by skilled linguists, although computational methods for detecting cognate pairs are emerging (Kondrak, 2001; Lefever et al., 2020; St Arnaud et al., 2017).

An interesting aspect of TDA on word embeddings is that it makes no assumption or use of translation pairs, surface similarities between words, or cognate pairs. Word embeddings are treated as *unlabeled* sets of points, shorn of any binding to corresponding tokens. TDA compares the relative *shape* of word embeddings in terms of structural properties like components of connectivity and holes.

Findings of the Association for Computational Linguistics: EMNLP 2024, pages 12080–12099
November 12-16, 2024 ©2024 Association for Computational Linguistics

That we demonstrate even a weak ability to reconstruct language phylogenies through TDA is quite surprising, and suggests that there are hitherto unknown structures reflected in word embeddings that go beyond the semantics of individual words.

Our major contributions in this paper include:

Further evidence that even within the Indo-European family the non-isometry between unlabeled word embeddings is not completely erroneous. The fact that we reconstruct phylogenetic trees that, despite not very precise, are considerably better than chance, suggests that there is some real information represented in the differences between unlabeled shapes of embeddings. It is fair to argue that more careful training, normalization and lemmatisation could yield more similar embeddings that miss the information; were that the case, it would suggest that the differences mitigated by those processes correlate with language history, which is an equally interesting observation.

A case study of natural generalizations of previously used methods to quantify non-isometry. TDA provides a relatively new set of tools for data science able to capture features often missed by more traditional approaches. Due to the general framework it provides, there are many parameters to choose from and a priori no obvious canonical choices. Our analysis on word embeddings represents a rigorous evaluation for an interesting use-case of this technology.

A particular instance of TDA was used in Patra et al. (2019); Vulić et al. (2020) as an approximation (Chazal et al., 2009) of difficult-to-compute Gromov-Hausdorff distance to quantify non-isometry of word embeddings. In the TDA terminology, they computed *bottleneck distance between degree* 0 *persistent diagrams*—we additionally explore degrees 1 and 2, and three different distances in addition to bottleneck; each combination for both Euclidean and cosine metric on the word embedding. Altogether this totals to 24 different combinations of parameters, and for each we obtain a distance matrix between the studied languages. All those notions of distances are invariant under orthogonal transformations[1], and therefore serve as quantifications for non-isometry. The alternative combinations can be better suited for studying word embeddings, e.g., by being less prone to irrelevant outliers that can artificially significantly increase the GH distance. Our analysis also shows that degree 2, which is not that often used in large high-dimensional data because of the expense in constructing them and difficulty to interpret them, yield statistically-strong results in our experiments, in some cases outperforming degrees 0 and 1.

Statistical Evaluation of TDA-Based Language Distances with Phylogenetic Trees. Evaluating the information content of language distance matrices inferred using TDA is best done by converting these matrices into phylogenetic trees, and then assessing the quality of these trees against a reference standard. Each of 24 different TDA matrices, constructed based on different combinations of parameters, was evaluated on two popular tree construction algorithms—UPGMA and neighbor joining—and compared against a gold-standard language tree from Ethnologue under six different tree-similarity metrics.

Certain choices of parameters prove less capable of recognizing the structural similarities inherent in word embeddings. But permutation tests show that for 484 out of 864 combinations of parameters[2], the quality of the reconstructed trees were significant to the 0.05-level, and many substantially stronger than that. Even stronger bounds come in the number of standard deviations our TDA trees are closer to the gold-standard tree compared to the mean statistical background. Many of our TDA-based trees sit from four to seven σ from the mean. Under assumptions of normality, the maximum achieved 6.87σ corresponds to a Bonferroni-corrected p-value of 2.77×10^{-9} of seeing a result like this by chance.

We presume a reader from computational linguistics, with a basic familiarity with the concepts and literature of word embeddings and language phylogenies, but no prior exposure to topological data analysis. Our paper is organized as follows. Important TDA concepts like persistence diagrams are reviewed in Section 2. Algorithms for constructing language phylogenies from distance matrices and evaluating the resulting trees are presented in Section 3. We describe our TDA-based analysis pipeline in Section 4 with computational results reported in Section 5, and conclude with Section 6.

Our primary goal in this work is to initiate the study of the shape of languages via word embed-

[1] Cosine distances can change with translation—a shift of the whole point cloud.

[2] See Section 4 for a break-down of the $864 = 2{\cdot}3{\cdot}4{\cdot}3{\cdot}2{\cdot}6$ combinations of parameters.

dings, *not* to advance the state-of-the-art in language phylogeny reconstruction. Indeed, cognate-based analysis should clearly dominate our unlabeled point methods except perhaps in pathological situations, such as completely undeciphered written languages. But we do believe that the new TDA-based tools hold promise for richer computational language analysis, and raise interesting questions about which properties in language-space the topological features we employ correspond to.

2 Topological Data Analysis

Topological data analysis (TDA) is a growing field that applies methods developed for studying shapes to data, both geometrical and abstract, to extract features that are often not captured by classical approaches of data science. In the case of points or vectors in 2D or 3D, we observe patterns like clusters of points, loops, voids or tunnels.

In this paper, the input is a word embedding of a language—collection of points in high-dimensional Euclidean space, one for each token—and the output is a summary of its topological features. We compute such summaries for embeddings of different languages, and use them to compare the structural similarity. As orthogonal transformations would preserve the summaries, those differences quantify non-ismoetry of the different embeddings.

To keep the explanation intuitive, we stay with low dimensional point sets, but the general framework is limited neither by dimension of the data nor by the Euclidean metric—indeed, we use 300-dimensional word embedddings and impose both Euclidean and cosine metrics. For a gentle introduction to TDA see Edelsbrunner (2014). For more technical details, see Edelsbrunner and Harer (2010). For applications of TDA to a wide variety of real-world data, see the database of non-theoretical uses of topology (Giunti et al., 2022).

2.1 Persistent Homology

We describe the idea of persistent homology in a simple intuitive setting—a data set of points in a Euclidean plane. To define the 'shape' of such a set, choose a radius, place a disk of that radius centered at each point, and consider the union of the disks; see Figure 1. Two simple descriptors for such a shape are the number of connected components and the number of holes—*Betti numbers*[3] β_0 and β_1, respectively. The notion is formally defined by *homology* from the mathematical field of algebraic topology; see, e.g., Hatcher (2002).

For different radii of the disks, we get different Betti numbers. Consider growing the radius from zero to infinity. We can plot the Betti numbers depending on the radius, and treat the curves, $\beta_0(r)$, $\beta_1(r)$, as descriptors for the shape of our point set. The problem is that such a curve can differ a lot when we slightly perturb the points. For a stable descriptor, we turn to *persistent homology*, which, in addition, pairs the *birth* and *death* radii of each component or hole. Components are all born at radius 0 and each time two components merge at radius r, we get a birth-death pair $[0, r)$. For a hole or a loop, there is a minimum birth radius, r_b, for which the disks enclose a space in the plane, separating it from its surroundings, and there is a larger minimum death radius, r_d, for which the area we previously enclosed is fully covered by the disks. The interval $[r_b, r_d)$, often called a *bar*, is a single feature recorded by persistent homology. It is the interval of radii during which this particular hole contributes "plus one" to the corresponding Betti number.

We collect all such intervals. Each interval is described by its two endpoints, so we can plot them all in a scatter plot with axes "birth radius" and "death radius"; see Figure 1(c). This plot is the *persistence diagram* of the data. For a point set in a plane, we get two persistence diagrams: one for components of connectivity—degree 0—and one for 'holes' or 'loops'—degree 1. Usually we plot both in the same figure, separating them by color or shape of the markers.

When we increase the dimension of the data, we can have more different kinds of features. In 3D, we grow balls rather than disks around the points. A degree 2 feature is an uncovered space completely surrounded by covered space—like a hole completely inside a Swiss cheese. A degree 1 feature is a loop drawn into the union of the balls that cannot be contracted to a point within that union. As loops in 3D, a 2-dimensional feature in higher dimensional data would not be a completely enclosed space, but rather a drawing of a 2-dimensional sphere that cannot be contracted to a point.

Although our actual data is 300-dimensional, we only consider features of degree 0, 1 and 2, mainly for computational reasons. Examples of diagrams from our analysis are in Appendix Figure 9.

[3] The formal definition of Betti numbers depends on the choice of coefficients for homology. We use the field of size two, which is the standard choice for persistent homology.

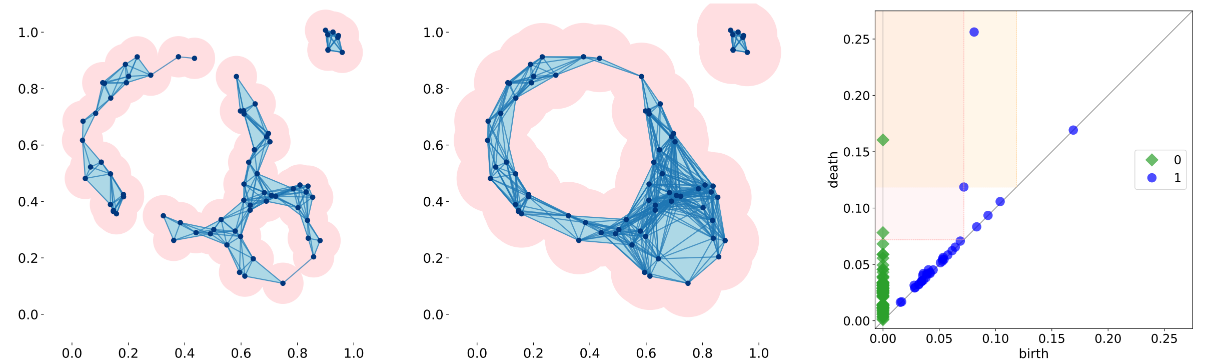

Figure 1: Unions of disks centered at data points in a Euclidean plane define a 'shape' that varies with the radius of the disks. In our setting, each point is one token of a word embedding, and the space is $\mathbb{R}^{300}$ rather than $\mathbb{R}^2$. Persistent homology studies different types of 'gaps' within this growing shape—0-dimensional gaps between components of connectivity, and 1-dimensional holes within the shape. Each such feature is born at some radius, and dies at some later radius, spanning an interval $[r_b, r_d)$. Those intervals are summarised in a persistence diagram; each interval is represented by a dot with coordinates (r_b, r_d). The *left* and *middle* figures correspond to birth and death radii of the loop in the lower-right corner: $[r_b, r_d) = [0.072, 0.119)$. Overlaid is the Vietoris-Rips complex discretizing the pink shape to allow for computations (see A.1). On the *right* is the persistence diagram of the growing disks with highlighted blocks corresponding to radii r_b, r_d.

Persistent homology is stable against perturbations. That is, if the data points are perturbed a bit, the points on the persistence diagrams are also only perturbed a bit (Cohen-Steiner et al., 2007). Note that in contrast, it is not very stable against outliers, which is a limitation of the tool that can be somewhat mitigated with the right choice of distance between persistence diagrams.

2.2 Distances Between Persistence Diagrams

In this section, we describe several established notions of distances between persistent diagrams. The list we use is by no means exhaustive—see, e.g., Ali et al. (2023) for a survey of methods, and Carrière et al. (2020) for an approach unifying many of those methods under a common framework. We chose four distances that are widely used in theory or in applications and have readily available implementations. Two of those are defined directly on the diagrams, while the other two first vectorize each diagram and then compare the vectors with the standard Euclidean metric. Note two properties that make defining distances somewhat involved: firstly, different persistence diagrams have generally different number of points with no canonical matching between them; secondly, slightly perturbing data can create or remove points at the diagonal, which needs to be taken into consideration.

We fix two persistent diagrams, PD_1 and PD_2, describing topological features of the same degree. An element r of PD_i is a point in a plane representing an interval, and we will denote its endpoints by $r = [r_b, r_d)$ for "birth" and "death".

Bottleneck distance. The first distance that was proved to be stable (Cohen-Steiner et al., 2007) is the *bottleneck distance*, which is defined as "the biggest difference for the best matching". A *matching*, $\mathcal{M}$, between two persistence diagrams is a pairing of the points they contain, with an added flexibility—we can match points with any points on the diagonal. That is, if $(r, s) \in \mathcal{M}$, then either $r \in \mathrm{PD}_1$ and $s \in \mathrm{PD}_2$ or only one of those holds and the other element is $[x, x)$ for some number x. The bottleneck distance between PD_1 and PD_2 is then

$$W_\infty(\mathrm{PD}_1, \mathrm{PD}_2) = \inf_{\mathcal{M}} \max_{(r,s)\in\mathcal{M}} \max\{|r_b - s_b|, |r_d - s_d|\}.$$

Bottleneck distance is a classical notion, but it is computationally costly since we have to search the space of matchings. It is comparing the similarity of the diagrams "on the nose". This is well-suited for those applications in which objects are considered similar only if their "hole-structure" is almost identical, but can be too penalising when we are interested more vaguely in the distribution of different kinds of holes. It is also very sensitive to outliers.

(Sliced) Wasserstein distance. The maxima in the bottleneck distance can be seen as l_∞-norm, which suggests that they can be replaced by l_p norms, for various $p \in \mathbb{N}$, to get different notions of distances. In particular, replacing both maxima by l_1-norm, we get 1-*Wasserstein distance* between persistence diagrams:

$$W_1(\mathrm{PD}_1, \mathrm{PD}_2) = \inf_{\mathcal{M}} \sum_{(r,s)\in\mathcal{M}} |r_b - s_b| + |r_d - s_d|$$

This distance takes each interval in either diagram into consideration, not just the worst match as the bottleneck distance. For discussion on stability with respect to data perturbations see Cohen-Steiner et al. (2010); Skraba and Turner (2023). In our analysis, we use a computationally more viable variant—*sliced Wasserstein distance* which approximates 1-Wasserstein distance (Carrière et al., 2017).

Persistence image. Rather than directly comparing the diagrams, we can first transform each into a vector and then compare the vectors. One approach to vectorize a diagram is to blur the points and then treat the plot as a raster image, called *persistence image* (Adams et al., 2017). Persistence images are stable and approximate the 1-Wasserstein distance. More formally, we put a two-dimensional Gaussian over each dot in the persistence diagram, and consider their sum. Then we overlay a grid over the domain, and compute the integral of the sum of Gaussians over each grid square. This yields a value for a pixel. Since the dots further away from the diagonal are more relevant, there is a weight function defining the height of the Gaussian based on the distance away from the diagonal. The distance between two diagrams is then the Euclidean distance between their persistence images viewed as vectors.

Persistence images are easy to compute, but there is several parameters we need to fix—the size of the pixels and the grid, the σ-parameter of the Gaussians, and the weight function controlling the heights of the Gaussians based on the distance from the diagonal.

Bars statistics. A somewhat naive, but surprisingly successful vectorization is to collect several simple statistics of the collection of dots (also called bars) in the persistence diagram (Pun et al., 2022; Cang et al., 2015; Ali et al., 2023). We used 40 numbers—10 statistics for 4 values. For each dot, (b, d), the 4 values are birth, death, persistence and midpoint, i.e., b, d, $d - b$ and $\frac{d+b}{2}$, respectively. The 10 statistics are: median, standard deviation, interquartile range, full range, 10th percentile, 25th percentile, 75th percentile, 90th percentile, and entropy. To compare two diagrams, we compute the Euclidean distance between the vectorizations.

This vectorization method misses theoretical guarantees like the stability, but is very easy to compute, the meaning of the features is clear, and may mitigate the negative effects of outliers.

3 Constructing Phylogenetic Trees

To evaluate whether the distances between languages calculated based on persistence homology are relevant, we use this data to attempt to reconstruct the historical evolution of Indo-European languages. We perform a hierarchical clustering, obtain a phylogenetic tree, and compare this tree to a ground-truth reference tree.

We emphasize that reconstructing language phylogenies is not the goal of our analysis, but rather we use it as a tool to evaluate whether the computed distances carry a relevant signal, meaning the unlabeled topological "shape" of word embeddings retain and reflect broader properties of the underlying languages. Phylogeny reconstruction is an enormous area within computational linguistics, and space does not permit us to make a substantial survey of work in this field. See Dunn (2015); Pereltsvaig and Lewis (2015); Pompei et al. (2011) for recent reviews of this literature.

In this paper, we experiment with two popular agglomerative hierarchical clustering algorithms for reconstructing phylogenetic trees from a pairwise distance matrix, $d(\cdot,\cdot)$. We start with each language as an individual cluster, and then we connect two closest clusters in each step. The difference is what "closest" means for each of the algorithms:

Unweighted Pair Group Method with Arithmetic Mean (UPGMA). The UPGMA method (Sneath and Sokal, 1973) approximates distances between clusters as the average distance between the elements: for clusters A, B, the distance is

$$d(A, B) := \frac{1}{|A| \cdot |B|} \sum_{\substack{a\in A \\ b\in B}} d(a, b).$$

Starting with singleton clusters, in each step it merges the two closest clusters into one.

Neighbor Joining (NJ). The NJ method (Saitou and Nei, 1987) defines distances between clusters,

$D(\cdot,\cdot)$, inductively through a merging process. Let C be the collection of current clusters. For each cluster, $a \in C$, define

$$\alpha(a) := \frac{1}{|C|-2} \sum_{\substack{b \in C \\ b \neq a}} D(a,b).$$

In each step, find a pair $a, b \in C$ minimizing $D(a,b) - \alpha(a) - \alpha(b)$. Then replace a, b by the union, $a \cup b$, and define the new distances $D(a \cup b, c) := (D(a,c) + D(b,c) - D(a,b))/2$ for each other c. The length of the new tree edge, $(a \cup b, a)$ is defined as $D(a,b) + \alpha(a) - \alpha(b)$, and symmetrically for $(a \cup b, b)$.

4 Analysis Pipeline

This section details the data, the process of going from the data to trees, and finally the evaluation of the reconstructed trees. Our code for the analysis is published on GitHub.[4]

4.1 Data

Our study requires two types of data over a large set of languages: (a) a source of directly comparable, high quality word embeddings, and (b) a ground-truth reference phylogenetic tree reflecting the origin and relative similarity of languages in this set. We limit our attention here to the broad family of Indo-European languages for this study.

The historical origin of languages has been extensively studied, and much is known, but debate remains vigorous even for the Indo-European languages we study here (Gray and Atkinson, 2003; Pereltsvaig and Lewis, 2015; Longobardi et al., 2013). The reference tree we use comes from Ethnologue[5], which is the most widely consulted inventory of the world's languages (Lewis et al., 2024). First published in 1951 and now in its 26th edition, Ethnologue currently records data about 7,168 living languages. Although there is no universal agreement on language origins (see e.g. Hammarström (2015) for a critique of Ethnologue), it provides a broadly acceptable reference tree for our evaluation purposes, particularly for the major Indo-European languages we consider here. One downside of this reference is the lack of weights on the edges of the tree—we only get the topology. An alternative for a follow-up research could be to compare to other computationally reconstructed trees that are considered reliable, e.g., Serva and Petroni (2008).

FastText[6] (Grave et al., 2018) provides a set of pre-trained, 300-dimensional word embeddings for 157 languages, trained on Common Crawl and Wikipedia. There are 81 Indo-European languages that appear in the Ethnologue reference tree and also have pre-computed FastText embeddings. To protect against the risk that low-resource languages might have less reliable embeddings, we will also evaluate filtrations to the most popular 30 and 50 languages. The Ethnologue reference trees for all filtrations are provided for inspection in Appendix Figure 7.

4.2 From Language Embeddings to a Tree

In this section we describe our pipeline to go from the embeddings of languages to a phylogenetic tree, list the parameter choices at each step, and provide details about the implementation.

We start with a set of embeddings of languages. For each language, we compute a distance matrix between its words. For each such matrix, we use persistent homology and get a set of persistent diagrams. Computing distances between the persistent diagrams yields a distance matrix labeled by languages. From this language distance matrix we finally construct a phylogenetic tree.

Language embeddings. As described in Section 4.1, we work with language embeddings from FastText. We filter the data in two ways. Firstly, we use the $V = 10{,}000$ most frequent tokens of each language—a threshold chosen to be as high as possible considering computational feasibility[7]. Secondly, we only choose a subset of the languages to work with. Because low-resource languages may skew our analysis, we filter the languages by the number of Wikipedia articles[8], and consider the first 30, 50 or all 81 available Indo-European languages.

Token-to-token distance matrices. As input to the persistent homology pipeline we use, for each language, we generate a $V \times V$ matrix, each entry being the distance between two 300-dimensional vectors, u, v. We use two differ-

[4] https://github.com/OnDraganov/shape-of-word-embeddings

[5] https://www.ethnologue.com

[6] https://fasttext.cc/

[7] Degree 2 PH is expensive; for 0 and 1, V can be increased.

[8] https://meta.wikimedia.org/wiki/List_of_Wikipedias, extracted on November 8, 2023

ent notions of distances: either the standard Euclidean distance, $||\, u - v\, ||$, or the cosine distance, $1 - a \cdot b\, /\, (||\, a\, || \cdot ||\, b\, ||)$, which is often used in language processing.

Persistence diagrams. For the token-to-token distance matrix of each language, we compute the persistence diagram[9] as described in Section 2, using an efficient implementation of this computation, `Ripser`[10] (Bauer, 2021). In this step, we choose the degree of the topological features to use—either 0, 1 or 2.

Languages distance matrix. From the set of persistence diagrams, we get a single distance matrix representing the proximity of language pairs. The distance between diagrams is one of the four described in Section 2.2—this is the fourth parameter.

We use bottleneck distance implementation from `GUDHI` library[11] (François, 2016), and slice Wasserstein and persistence image implementations from `persim` Python library[12]. Bar statistics are computed directly.

Persistence images take several parameters. Our choices depend on the embedding metric used and persistence diagram degree considered. For degrees 1 and 2 we use a 10×10 grid. For degree 0 it is just 1×10 grid. The range of radii covered by the grid is $[0, 10]$ for Euclidean embedding metric, and $[0, 1]$ for cosine. Note that if there is a dot outside of this range in the persistence diagram, the Gaussian is still put over it, and spills into the considered range, so even those dots are still considered in the distance. The weight function is linear in all cases, $w(d - b) = d - b$. Careful optimization of these parameters might lead to better results.

For the bars statistics, in degree 0 we only use the death, d, value, as $b = 0$ for all dots. That is, the vectorization is 10-dimensional in this case rather than 40-dimensional as in the other cases.

Tree construction. Finally, we construct a phylogenetic tree based on the language distance matrix. We try two different approaches. We use either of the two agglomerative clustering algorithms described in Section 3—neighbor joining (NJ) or unweighted pair group method with arithmetic mean (UPGMA). Both of those algorithms are implemented in `biopython` package[13] under `DistanceTreeConstructor` class. Figure 8 in Appendix gives examples of reconstructed and reference trees.

Two aspects of this approach make comparisons of thus reconstructed trees to the reference difficult. Firstly, the reference Ethnologue tree has no weights on edges, so we cannot meaningfully use the weights of the reconstructed trees either. Secondly, the Ethnologue tree is flat and neither binary nor rooted, while the reconstructed trees are generally somewhat deep binary trees. Our solution to this difference in topology is to test the reconstructed trees against their copies with permuted leaf labels.

We also conducted a second set of experiments to allay the concerns about the difference in height and topology between reconstructed and reference trees. We fix the topology of the reference Ethnologue tree, and try to assign languages to the leaves—to do that, we optimise the similarity of the path-distance matrix given by the labeled tree to the distance matrix computed using TDA. We then evaluate this optimized labeling against 100,000 random labelings. Consistent with the results reported below, we perform substantially better than chance for almost all combinations of parameters, typically by two or more standard deviations from the mean. Details of this alternative analysis are presented in the Appendix (A.2).

Summary of the parameters. To construct one tree we choose a number of languages (30, 50, 81), an embedding (Euclidean, cosine), a degree of persistence diagrams (0, 1, 2), a distance between persistence diagrams (bottleneck, sliced Wasserstein, persistence image, bars statistics), and a construction of a tree (UPGMA, NJ)—altogether $3 \cdot 2 \cdot 3 \cdot 4 \cdot 2 = 144$ variants. For each there are six tree distances to evaluate how well we reconstructed the phylogeny, as described below.

4.3 Evaluating Phylogenetic Trees

To compare the reference Ethnologue tree E to each phylogenetic tree T constructed using the language distances inferred by TDA, we employ six different tree distances, using implementations from the `R` package `TreeDist` version `2.6.3`. These include (i/ii) Jaccard-Robinson-Foulds distance for $k = 1$ and $k = 2$ (Nye et al., 2005; Böcker et al., 2013), (iii) matching split distance (Bogdanowicz and Giaro, 2012; Lin et al., 2012), (iv/v) the phylogenetic and clustering information

[9] We use Vietoris-Rips complex, described in Section A.1.

[10] `https://github.com/Ripser/ripser`

[11] `https://gudhi.inria.fr`

[12] `https://github.com/scikit-tda/persim`

[13] `https://biopython.org/wiki/Phylo`

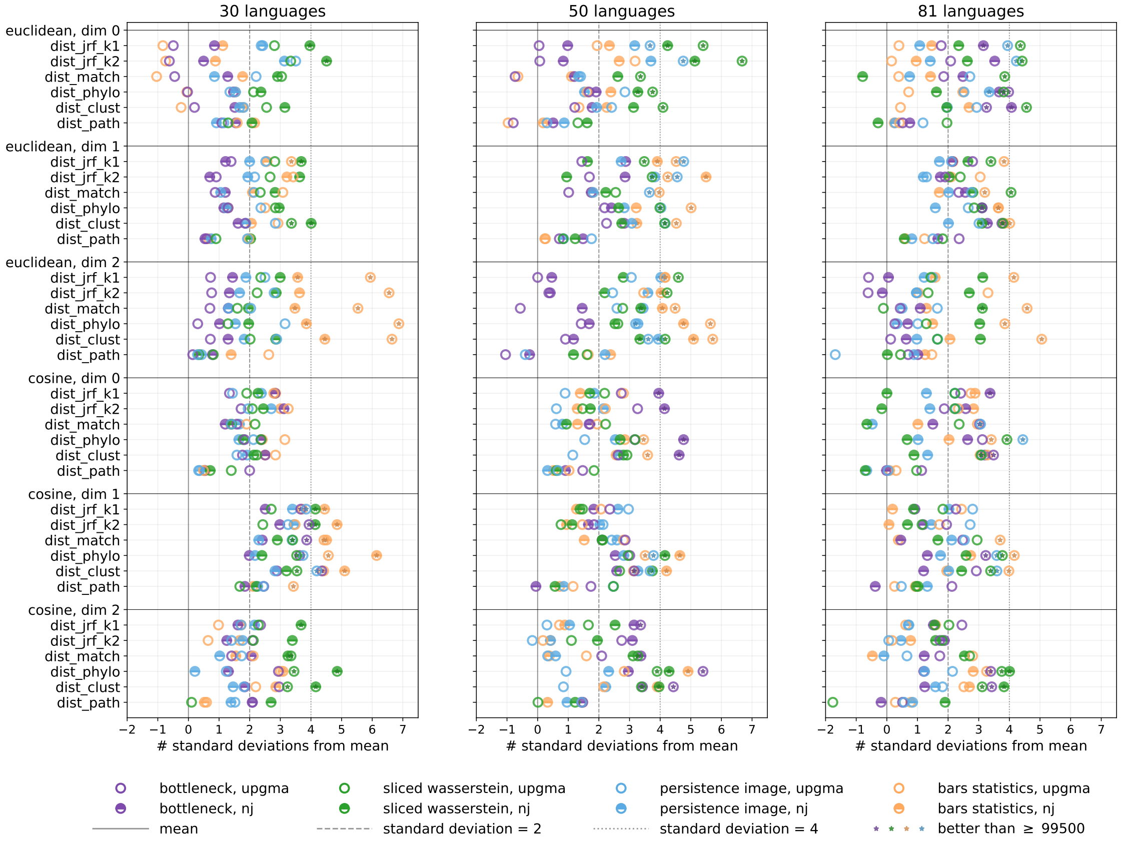

Figure 2: The statistical significance of TDA trees for 30, 50, and 81 languages against the Ethnologue reference, E, for trees reconstructed by UPGMA and NJ for each combination of parameters described in Section 4. Each dot represents a single reconstructed tree, T, and a tree distance, D. We performed 100,000 random permutations of the leaves of T, and compared each to the reference E using the distance D. This yields a distribution with mean μ and standard deviation σ. To evaluate the reconstruction T, we plot $(\mu - D(T, E))/\sigma$. The higher the value, the better the reconstruction. A star inside a dot signifies that $D(T, E)$ is smaller than 95,500 of the permuted tree distances.

distances (Smith, 2020), and (vi) path distance (Farris, 1969; Steel and Penny, 1993). We provide detailed descriptions of these distances in Appendix Section A.3.

To assess whether the reconstructed trees capture part of the real phylogeny, we evaluate them in terms of leaf label permutations—comparing the distance $d(T, E)$ between the algorithmic tree T and reference E to the distribution of $d(T', E)$, where T' is obtained from T by shuffling the leaf labels.

For each of the 144 constructed trees, T, we performed 100,000 permutations of its leaf labels. For each permuted tree, we measure the six tree distances to the reference Ethnologue tree with the corresponding number of leaves—30, 50 or 81. Then, separately for each of the six tree distances, we identify where in this distribution of distances $d(T, E)$ lies. The measure of success is to check how many random permutations did worse than T.

5 Results of the Experiments

The experiments show correlation between the word embedding dissimilarity and language phylogeny—for 484 out of 864 distributions, at least 95,000 (95%) of the permutations are further from the reference tree E than the reconstructed tree T is.

Figure 2 is the primary result in this paper, presenting the results of evaluations of 144 different tree reconstructions based on TDA, each evaluated on six different tree similarity measures, for a total of 864 different points. By employing permutation tests, we can map each such point to a significance level, expressed in terms of (a) the fraction of random samples dominated by the reconstructed tree or (b) the number of standard deviations the reconstructed tree sits from the mean value over 100,000 permutations of leaves; the options are tightly correlated. Figure 2 summarises (b); analogous figure for (a) is in Appendix Figure 6.

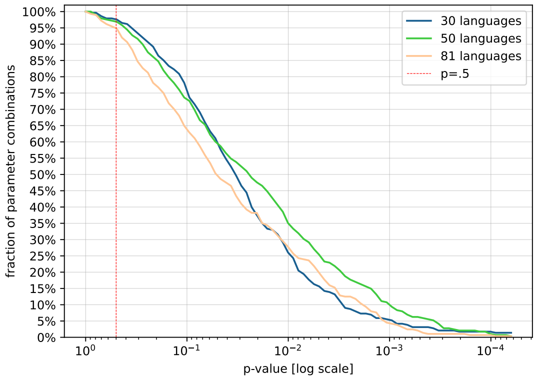

Figure 3: The fraction of parameter combinations (out of 288) in Figure 2 bested by $\leq p{\cdot}100{,}000$ permutations.

Further summary of these results is in Figure 3. The cumulative distribution plots show the fraction of experimental conditions which satisfy a given permutation test p-value. With respect to this value, 484 out of the 864 conditions proved significant to at least the 0.05-level. Of these, 255 were significant to at least 0.01, 57 to at least 0.001, and 10 to 0.0001. In one case the algorithmic tree dominated all $t = 100{,}000$ random permutations evaluated.

Our statistically strongest results came when using 50 languages: possibly large enough to encode topologies hard to find by chance while avoiding low resource languages with poorly shaped embeddings. Twice as many tests for UPGMA trees (114) were significant to the 0.005-level as NJ trees (63), demonstrating that better combinatorial optimization leads to more significant phylogenies.

Different distances between persistent diagrams seem to fit well with different degree and token-to-token metric. Overall, bars statistics and sliced Wasserstein seem to perform better, while bottleneck is the least successful—this might be explained by its strong sensitivity to outliers, and suggests that the other notions might be better suited for analyses of word embeddings' (dis)similarities. Detailed breakdowns of the success of different parameters are provided in Tables 1, 2, 3, 4 in the Appendix.

That our best tree beats all trial t permutations in our experiment implies it is significant beyond the $1/t$ level. By measuring the quality score of each tree with respect to each distance in terms of the number of standard deviations above its random background mean and assuming normality, we can obtain a p-value associated with each such z-score. The maximum achieved 6.87σ corresponds to a Bonferroni-corrected p-value of $2.77 \times 10^{-9} = P\left[x \geq 6.87\right] * 864$, assuming a normal distribution. Coupled with all other presented permutation test results, clearly TDA is picking up real signal from the shape of word embeddings.

6 Conclusions

Our analysis of FastText word embeddings of 81 Indo-European languages suggests that deviations from pair-wise isometry correlates with the historical origin of the languages—an interesting contribution to the debate about the extent to which the variance between monolingual embeddings is explained by essential differences between the languages versus scarcity of resources and undertraining when constructing them.

A natural question is to what extent the presented results generalize. Would we get comparably significant results for word embeddings trained with different algorithms, with different parameters or on a different corpus? And if more careful training should lead to isometric embeddings, as suggested by Vulić et al. (2020), is there an explanation for a correlation of lower quality of embeddings with language phylogeny?

The results suggest that TDA methods can help us better understand the structure of word embeddings, and further research can lead to useful insights. Different parameters can be better suited for comparing word embeddings than the previously used bottleneck lower bound of Gromov-Hausdorff distance. Furthermore, better understanding of the particular detected topological features could lead to interesting insights. For example, looking at a single language embedding, we can look back at concrete loops in degree 1 persistence diagrams and ask whether the collection of words it passes through has some meaningful linguistic interpretation. Or, identifying a large loop in one language, we can ask whether the translation of the words also forms a large loop in other languages.

Limitations

In this paper, we have demonstrated that TDA methods are capable of reconstructing a real (albeit somewhat weak) signal about language structure and history from unlabeled word embeddings.

However, there are reasons to be optimistic that the strength of this signal may be increased with further research and experience. We note that our TDA analysis is "blind", with no statistical normalizations of numerical range across the different language embeddings. Orthogonal transformations preserve distances and angles, so they do not influence persistent homology, but scaling does change Euclidean distances, and translation (shifts) can change the cosine distances.

Outlier points may impact persistent homologies in misleading ways. For example the "U-" token in the English language embedding skewed the Euclidean 0-dim homology, even though it was completely isolated. This motivates the question of whether we can preprocess data to eliminate clear outliers before analysis.

There is somewhat of a gap between the low-dimensional persistent homologies of dimensions $0 \leq d \leq 2$ which are computationally accessible and the 300-dimensional word vectors we analyze. In hopes of capturing more of the higher order behavior of high-dimensional data, data is often first reduced to fewer dimensions before persistent homology is applied. Standard methods like PCA, t-SNE or U-Map can be used to reduce dimensionality to ~ 10 or ~ 50.

We restrict our attention here to one popular but particular set of GloVe embeddings, without evaluating other methods such as word2vec, which are geometrically quite different and may in principle have even better topological properties. There are also reasonable questions of whether our results may strengthen if we used a different reference tree than provided by Ethnologue which is difficult to compare to: it is unrooted, non-binary, and very flat.

The phylogeny of languages might also not be the aspect most correlated with the distances we see. For example geographical and structural similarities as studied in Bjerva et al. (2019) could lead to closer correlations.

Our results demonstrate that TDA invariants capture properties of languages, but what aspects of language are they keying on? What do tunnels and voids in embeddings tell us about languages?

References

Henry Adams, Tegan Emerson, Michael Kirby, Rachel Neville, Chris Peterson, Patrick Shipman, Sofya Chepushtanova, Eric Hanson, Francis Motta, and Lori Ziegelmeier. 2017. Persistence images: A stable vector representation of persistent homology. *Journal of Machine Learning Research*, 18.

Dashti Ali, Aras Asaad, Maria-Jose Jimenez, Vidit Nanda, Eduardo Paluzo-Hidalgo, and Manuel Soriano-Trigueros. 2023. A survey of vectorization methods in topological data analysis. *IEEE Transactions on Pattern Analysis and Machine Intelligence*, 45(12):14069–14080.

Ulrich Bauer. 2021. Ripser: efficient computation of Vietoris-Rips persistence barcodes. *J. Appl. Comput. Topol.*, 5(3):391–423.

Johannes Bjerva, Robert Östling, Maria Han Veiga, Jörg Tiedemann, and Isabelle Augenstein. 2019. What do language representations really represent? *Computational Linguistics*, 45(2):381–389.

Sebastian Böcker, Stefan Canzar, and Gunnar W. Klau. 2013. The generalized Robinson-Foulds metric. In *Algorithms in Bioinformatics*, pages 156–169, Berlin, Heidelberg. Springer Berlin Heidelberg.

Damian Bogdanowicz and Krzysztof Giaro. 2012. Matching split distance for unrooted binary phylogenetic trees. *IEEE/ACM Transactions on Computational Biology and Bioinformatics*, 9(1):150–160.

Zixuan Cang, Lin Mu, Kedi Wu, Kristopher Opron, Kelin Xia, and Guo-Wei Wei. 2015. A topological approach for protein classification. *Computational and Mathematical Biophysics*, 3(1).

Mathieu Carrière, Frédéric Chazal, Yuichi Ike, Théo Lacombe, Martin Royer, and Yuhei Umeda. 2020. Perslay: A neural network layer for persistence diagrams and new graph topological signatures. In *International Conference on Artificial Intelligence and Statistics*, pages 2786–2796. PMLR.

Mathieu Carrière, Marco Cuturi, and Steve Oudot. 2017. Sliced Wasserstein kernel for persistence diagrams. In *Proceedings of the 34th International Conference on Machine Learning*, volume 70 of *Proceedings of Machine Learning Research*, pages 664–673. PMLR.

Frédéric Chazal, David Cohen-Steiner, Leonidas J Guibas, Facundo Mémoli, and Steve Y Oudot. 2009. Gromov-Hausdorff stable signatures for shapes using persistence. In *Computer Graphics Forum*, volume 28, pages 1393–1403. Wiley Online Library.

David Cohen-Steiner, Herbert Edelsbrunner, and John Harer. 2007. Stability of persistence diagrams. *Discrete Comput Geom*, 37:103–120.

David Cohen-Steiner, Herbert Edelsbrunner, John Harer, and Yuriy Mileyko. 2010. Lipschitz functions have l_p-stable persistence. *Foundations of Computational Mathematics*, 10:127–139.

Michael Dunn. 2015. Language phylogenies. *The Routledge handbook of historical linguistics*, pages 190–211.

Herbert Edelsbrunner. 2014. *A Short Course in Computational Geometry and Topology*. Springer Cham.

Herbert Edelsbrunner and John Harer. 2010. *Computational Topology: An Introduction*. American Mathematical Society.

James S. Farris. 1969. A Successive Approximations Approach to Character Weighting. *Systematic Biology*, 18(4):374–385.

Godi François. 2016. Bottleneck distance. In *GUDHI User and Reference Manual*. GUDHI Editorial Board.

Barbara Giunti, Jānis Lazovskis, and Bastian Rieck. 2022. DONUT: Database of Original & Non-Theoretical Uses of Topology. `https://donut.topology.rocks`.

Edouard Grave, Piotr Bojanowski, Prakhar Gupta, Armand Joulin, and Tomas Mikolov. 2018. Learning word vectors for 157 languages. In *Proceedings of the International Conference on Language Resources and Evaluation (LREC 2018)*.

Russell D. Gray and Quentin D. Atkinson. 2003. Language-tree divergence times support the Anatolian theory of Indo-European origin. *Nature*, 426(6965):435–439.

Harald Hammarström. 2015. "Ethnologue" 16/17/18th editions: A comprehensive review. *Language*, 91:723–737.

Allen Hatcher. 2002. *Algebraic topology*. Cambridge University Press, Cambridge.

Grzegorz Kondrak. 2001. Identifying cognates by phonetic and semantic similarity. In *Second Meeting of the North American Chapter of the Association for Computational Linguistics*.

Guillaume Lample, Alexis Conneau, Marc'Aurelio Ranzato, Ludovic Denoyer, and Hervé Jégou. 2018. Word translation without parallel data. In *ICLR*.

Els Lefever, Sofie Labat, and Pranaydeep Singh. 2020. Identifying cognates in English-Dutch and French-Dutch by means of orthographic information and cross-lingual word embeddings. In *Proceedings of the Twelfth Language Resources and Evaluation Conference*, pages 4096–4101, Marseille, France. European Language Resources Association.

M. Paul Lewis, Gary F. Simons, and Charles D. Fennig. 2024. Ethnologue: The languages of the world. SIL International, Dallas.

Yu Lin, Vaibhav Rajan, and Bernard M.E. Moret. 2012. A metric for phylogenetic trees based on matching. *IEEE/ACM Transactions on Computational Biology and Bioinformatics*, 9(4):1014–1022.

Giuseppe Longobardi, Cristina Guardiano, Giuseppina Silvestri, Alessio Boattini, and Andrea Ceolin. 2013. Toward a syntactic phylogeny of modern Indo-European languages. *Journal of Historical Linguistics*, 3(1):122–152.

Antonio Valerio Miceli Barone. 2016. Towards cross-lingual distributed representations without parallel text trained with adversarial autoencoders. In *Proceedings of the 1st Workshop on Representation Learning for NLP*, pages 121–126, Berlin, Germany. Association for Computational Linguistics.

Tom M.W. Nye, Pietro Liò, and Walter R. Gilks. 2005. A novel algorithm and web-based tool for comparing two alternative phylogenetic trees. *Bioinformatics*, 22(1):117–119.

Barun Patra, Joel Ruben Antony Moniz, Sarthak Garg, Matthew R. Gormley, and Graham Neubig. 2019. Bilingual lexicon induction with semi-supervision in non-isometric embedding spaces. In *Proceedings of the 57th Annual Meeting of the Association for Computational Linguistics*, pages 184–193, Florence, Italy. Association for Computational Linguistics.

Asya Pereltsvaig and Martin W Lewis. 2015. *The Indo-European Controversy*. Cambridge University Press.

Simone Pompei, Vittorio Loreto, and Francesca Tria. 2011. On the accuracy of language trees. *PloS one*, 6(6):e20109.

Chi Seng Pun, Si Xian Lee, and Kelin Xia. 2022. Persistent-homology-based machine learning: a survey and a comparative study. *Artificial Intelligence Review*, 55(7):5169–5213.

D.F. Robinson and L.R. Foulds. 1981. Comparison of phylogenetic trees. *Mathematical Biosciences*, 53(1):131–147.

Naruya Saitou and Masatoshi Nei. 1987. The neighbor-joining method: a new method for reconstructing phylogenetic trees. *Molecular biology and evolution*, 4(4):406–425.

M. Serva and F. Petroni. 2008. Indo-European languages tree by Levenshtein distance. *Europhysics Letters*, 81(6):68005.

Primoz Skraba and Katharine Turner. 2023. Wasserstein stability for persistence diagrams. *arXiv*, page 2006.16824.

Martin Ross Smith. 2020. Information theoretic generalized Robinson–Foulds metrics for comparing phylogenetic trees. *Bioinformatics*, 36(20):5007–5013.

Peter H.A. Sneath and Robert R. Sokal. 1973. Unweighted pair group method with arithmetic mean. *Numerical Taxonomy*, pages 230–234.

Anders Søgaard, Sebastian Ruder, and Ivan Vulić. 2018. On the limitations of unsupervised bilingual dictionary induction. In *Proceedings of the 56th Annual*

Meeting of the Association for Computational Linguistics (Volume 1: Long Papers), pages 778–788, Melbourne, Australia. Association for Computational Linguistics.

Adam St Arnaud, David Beck, and Grzegorz Kondrak. 2017. Identifying cognate sets across dictionaries of related languages. In *Proceedings of the 2017 Conference on Empirical Methods in Natural Language Processing*, pages 2519–2528, Copenhagen, Denmark. Association for Computational Linguistics.

Mike A. Steel and David Penny. 1993. Distributions of Tree Comparison Metrics—Some New Results. *Systematic Biology*, 42(2):126–141.

Ivan Vulić, Sebastian Ruder, and Anders Søgaard. 2020. Are all good word vector spaces isomorphic? In *Proceedings of the 2020 Conference on Empirical Methods in Natural Language Processing (EMNLP)*, pages 3178–3192, Online. Association for Computational Linguistics.

Meng Zhang, Yang Liu, Huanbo Luan, and Maosong Sun. 2017. Adversarial training for unsupervised bilingual lexicon induction. In *Proceedings of the 55th Annual Meeting of the Association for Computational Linguistics (Volume 1: Long Papers)*, pages 1959–1970, Vancouver, Canada. Association for Computational Linguistics.

A Supplemental Material

A.1 Vietoris-Rips complex

To compute persistent homology, the continuous spaces of growing balls around the points in the cloud need to be replaced by a discrete structure easily represented in a computer. Concretely, by a simplicial complex, a (hyper)graph-like structure. A *simplicial complex* consists of a set of vertices, and a set of faces. Each face is a subset of vertices, and for each face, a simplicial complex has to also include all its subsets. A *filtration* of a simplicial complex is a function that assigns a real number to each face, and is monotone with respect to inclusion, that is, a subset of a face has to have smaller or equal value. A collection of all faces with value at most $r \geq 0$ is then a simplicial complex. This yields a chain of growing simplicial complexes.

For low-dimensional Euclidean data, persistent homology is usually computed using Delaunay complexes with alpha filtration. From the topological perspective, those complexes exactly reflect the spaces of growing disks. However, computing Delaunay complexes is not practically viable for data in dimensions beyond ~ 10. A widely used alternative is the Vietoris-Rips complex. It can be constructed from any distance matrix, and for Euclidean data offers a good approximation of the alpha filtration. Its low-dimensional persistent homology can be computed efficiently, and a fast implementation is readily available.

Given an $n \times n$ distance matrix D, and a radius $r > 0$, the *Vietoris-rips complex*, $\mathrm{VR}_r(D)$, is the flag complex of all the edges $\{i, j\}$ with $D_{i,j} \leq r$. That is, $\sigma \subseteq [n] = \{1, \ldots, n\}$ is a face of $\mathrm{VR}_r(D)$ iff $D_{i,j} \leq r$ for all $\{i, j\} \subseteq \sigma$. As the radius grows to infinity, the complex grows to become the full-simplex $2^{[n]}$ whose size grows exponentially with respect to n. The reason that this is not a problem for computations is that the full complex need not be computed to obtain persistent homology. Firstly, only edges, triangles and tetrahedra are relevant when we only care for 0-, 1- and 2-dimensional persistent homology, secondly, there exists a radius cut-off after which the homology is guaranteed to be trivial, and finally, the relevant structures can be used implicitly rather than stored explicitly in memory. For more details see (Bauer, 2021).

For completeness we provide the formal definition of a 'feature' within a VR complex. A boundary $\partial\sigma$ of a face $\sigma \in \mathrm{VR}_r(D)$ is the collection of subsets $\sigma \setminus \{i\}$ for each $i \in \sigma$. An addition operation is defined on boundaries as the symmetric difference of the collections. A boundary of a collection of faces is then the sum of their boundaries. For example, the boundary of two triangles sharing an edge are the four edges on the outside.

There is a bar $[r_b, r_d)$ in the p-dimensional persistence diagram of $\mathrm{VR}_\bullet(D)$ iff there exist two collections of faces, $\mathcal{B} \subseteq \mathrm{VR}_{r_b}(D)$ and $\mathcal{D} \subseteq \mathrm{VR}_{r_d}(D)$, with the following properties. First, the boundary $\partial\mathcal{B}$ is empty, and one of the faces in $\mathcal{B}$ appears for the first time in $\mathrm{VR}_{r_b}(D)$. Second, the boundary $\partial\mathcal{D}$ is $\mathcal{B}$, and one of the faces in $\mathcal{D}$ appears for the first time in $\mathrm{VR}_{r_d}(D)$. For example, a 1-dimensional bar means that an edge appears in r_b which completes a loop, and then this loop is filled by a collection of triangles, the last of which appears in r_d.

A.2 Preserving the Ethnologue Tree Topology

Our previous experiments compared algorithmically-constructed trees (UPGMA and NJ) built using TDA-based distance matrices against the Ethnologue reference trees on identical sets of languages. A possible objection to this approach is that the reference trees are generally much shallower than those constructed by the algorithms, perhaps affecting our evaluation.

Thus we investigated an optimization procedure to construct TDA-based trees consistent with the reference tree topology. Instead of constructing a new tree, we try to find the best assignment of labels (languages) to the leaves based on the given distance matrix. A tree always yields a distance matrix between the leaves—the distance of two leaves is the length of the unique path connecting them. We set up an optimization process to find the label assignment leading to the tree distance matrix that best correlates with our given distance matrix. To compare distance matrices, we use the Pearson correlation coefficient. Therefore, if E is the tree distance matrix of the Ethnologue tree, and D is the distance matrix computed from the pipeline as described above, we want to find a permutation matrix P that maximizes the Pearson correlation coefficient between $P^T EP$ and D.

This is, however, a difficult optimization problem. To compute the Pearson correlation, the entries in the matrices are first replaced by their ranks, leading to matrices E', D', and the coefficient is then the covariance $\mathrm{cov}(E', D')$ divided by the standard deviations. The collection of entries does not change when we permute the matrices, so we retain the same ranks, means, and standard deviations. This means that we search for P maximizing $\langle P^T E'' P,\, D'' \rangle_F$, where E'', D'' are the matrices whose entries are ranks minus the mean of ranks, and $\langle \cdot, \cdot \rangle_F$ is the Frobenius inner product, which is the standard scalar product of the matrices viewed as unraveled vectors. This is, however, an instance of the quadratic assignment problem, which is generally NP-hard.

Our search for an optimal permutation is a naive flip-heuristic. Starting with a random permutation, we try random transpositions, and keep them if they improve the correlation. This procedure gets stuck in a local optimum after a few thousand flips. For each distance matrix, we ran this process 100 times and took the maximum of the local optima.

Our results are presented in Figure 4. Consistent with the results reported previously, we perform substantially better than chance for almost all combinations of TDA variant and tree distance metric, typically by two or more standard deviations from the mean.

A.3 Tree Similarity Metrics

To evaluate the experimental results, we need to quantitatively compare phylogenetic trees built using topological data analysis against the reference language tree from Ethnologue. Many labeled tree-to-labeled tree distances have been defined in the literature. We chose six different distances in our analysis, considering meaningfulness in our setting, availability of implementation, and efficiency of computation.

Generally there are two main directions in comparing trees. One is to define some notion of distances between pairs of leaves—e.g., the length of the shortest path connecting leaves or the distances of the closest common ancestor to either the root or to the leaves—and compare the distance matrices. This approach is not particularly well suited for our application, as reference Ethnologue tree is very flat. Nevertheless, we include one such distance.

Path distance (Farris, 1969; Steel and Penny, 1993). A path distance matrix of a tree is labeled by the leaves, and an entry is the length of the unique path in the tree that connects the corresponding two leaves. The distance of two trees is then the Frobenius distance of their path distance matrices—that is, the Euclidean distance when the matrices are unraveled into vectors.

The other option is to compare the different ways that the tree can partition its leaves into two groups by removing an edge. The first and simplest such method is the Robinson-Foulds (RF) metric (Robinson and Foulds, 1981). The distance of two trees, T_1, T_2, with the same leaves, is the number of partitions achievable by T_1, but not T_2, plus the number of partitions achievable by T_2 but not T_1; possibly normalised to range from 0 to 1. Partitioning is intuitively a good way to measure success of our method—after all, when naively comparing a constructed tree to the reference, we argue with claims like "Slavic languages are well separated from the others". The problem with RF is that comparing partitions on the nose is too penalizing. For example with a single swap of Portuguese with Czech in the 30-language Ethnologue tree (Figure 7), we go from distance zero to more than half of the maximum. Even reasonably similar trees can often get the maximum distance.

To fix the issue, generalizations of RF metric quantify the similarity of any pair of partitions. To compute how similar two trees are, we find the matching of the partitions defined by T_1 with the ones defined by T_2 that maximizes the sum of similarities of the matched partitions. To go from similarity to distance, we take the difference of theoretically maximal similarity and the computed similarity, and normalize to fit in the range 0 to 1. All the distances below follow the same logic, but differ in the definition of the similarity between two partitions. For the explanations, consider A_0, A_1 a partition of the leaves obtained by removing an edge from the tree T_1, and B_0, B_1 another partition arising the same way from T_2.

Jaccard-Robinson-Foulds distance (Nye et al., 2005; Böcker et al., 2013). JRF is a family of distances with one parameter, k. Its name comes from using the Jaccard index: $J(A_i, B_j) := |\, A_i \cup B_j \,| / |\, A_i \cap B_j \,|$. The similarity of two partitions is defined as the bigger of the two values, $\min\left(J(A_0, B_0), J(A_1, B_1)\right)$ and $\min\left(J(A_0, B_1), J(A_0, B_1)\right)$, raised to the power k. As k tends to infinity, JRF distance converges to RF. In our analysis, we use $k = 1$ and $k = 2$.

Matching split distance (Bogdanowicz and Giaro, 2012; Lin et al., 2012). The matching similarity of two partitions is the maximum of $|\, A_0 \cap B_0 \,| + |\, A_1 \cap B_1 \,|$ and $|\, A_0 \cap B_1 \,| + |\, A_1 \cap B_0 \,|$. The idea is that the number of leaves minus the similarity is the number of leaves that need to be swapped in order to obtain identical partitions.

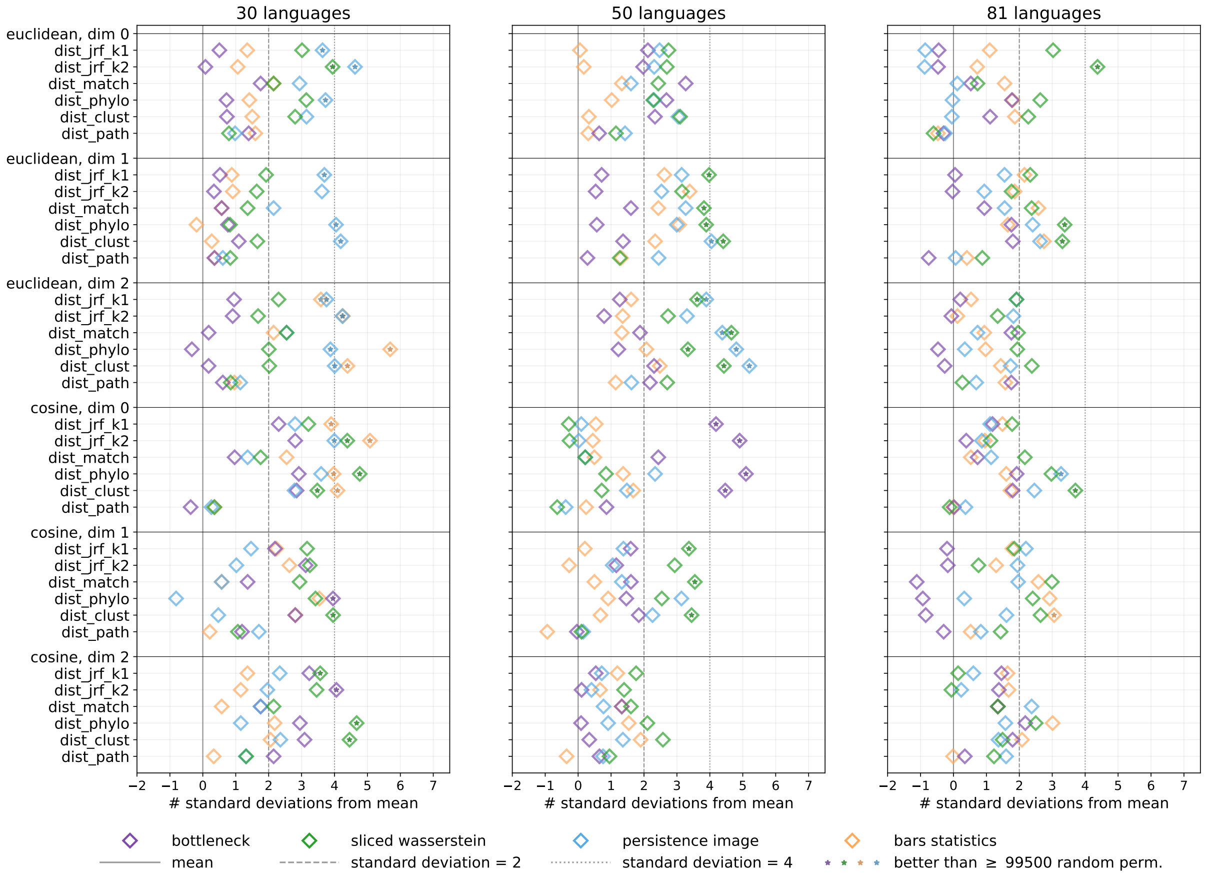

Figure 4: The statistical significance of the labelings of the Ethnologue tree that optimize distance matrix correlation (see Section A.2), for each combination of parameters described in Section 4. Each dot represents the distance of a single reconstructed labeling to the reference Ethnologue tree, and its position shows how many standard deviations away from the mean it lies in a distribution of 100,000 random labelings of the Ethnologue tree.

Phylogenetic and Clustering information distances (Smith, 2020). These metrics use notions from information theory to quantify similarity of partitions. The former measures the information in bits shared between the two partitions, while the latter quantifies the similarity with shared entropy.

For further details on both the intuition and the technicalities of the tree distances, see the documentation[14] of `TreeDist` package for `R`, which we used for the computations.

A.4 P-values from Permuting Labels

Although there exist many distance metrics for comparing rooted, labeled trees, these metrics can be difficult to interpret because they conflate differences in tree topologies (e.g height and width) with differences in leaf labelings (e.g. which label pairs are siblings of each other). In our experiments with language phylogenies, we observed that the toplogies of trees built from different heuristics (NJ and UPGMA) differed dramatically, and that both differed substantially in shape from both the reference tree and random trees constructed from natural agglomerative processes.

To evaluate the statistical significance of TDA-inspired trees, we propose the following procedure to mitigate impact of differing topology on our distance metrics. To evaluate how well an algorithmic tree (T) agrees with a given reference tree (R) with respect to a given distance metric $d(T, R)$, we construct a set of n random label-permuted algorithmic trees $T'(i)$, $1 \leq i \leq n$. These label-permuted trees will each have the exact same topology as T, but the leaf-labels of T be randomly and independently permuted in each $T'(i)$.

Comparing $d(T, R)$ to $d(T'(i), R)$ reflects only the differences in labeling while conserving topology. The degree to which T is better than the background of label-permuted can be assessed in two different ways. First, the rank r of the value

[14] https://ms609.github.io/TreeDist/reference/index.html

$d(T, R)$ against the universe of n label-permuted trees yields a p-value of $(r-1)/n$. Second, after computing the mean μ and standard deviation σ of the distribution of $d(T'(i), R)$, we can interpret $d(T, R)$ in terms of the number of standard deviations from the mean, which map directly to p-values assuming a normal distribution. We employ both techniques in the analysis to follow. The Spearman correlation of the two approaches is larger than 0.99, which indicates that we can use them interchangeably. We prefer the latter as it also takes the spread of the distribution into account, and can additionally identify meaningful p-values of statistical significance greater than $1/100{,}000$.

A.5 Significance Results

The result for the number of standard deviations from the mean are presented in Figure 5. Fully 451 out of 864 conditions yielded results that sat at least 2σ above the mean, with 229 at least 3σ, 74 at least 4σ, and five conditions at least 6σ above the mean, peaking at 6.87σ. For detailed breakdown see Table 3.

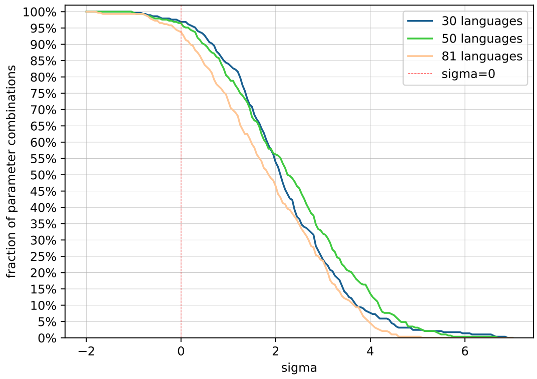

Figure 5: The fraction of parameter combinations (out of 288) in Figure 2 further away from the mean than σ standard deviations.

A.6 Evaluation of TDA Methods

To better understand which parameters perform the best, we aggregate the information from Figure 2 in two ways. In Table 1, we give the averages of standard deviations away from the mean when we fix some parameters and vary others, while in Table 2 we show the numbers of dots that performed better than 99.5% of the random permutations. In the first block of each table we compare metric for the word embedding and persistent homology dimension to compare the different distances. In the second block we compare the persistence diagram distance to compare how meaningful different topological features were. In the third block we compare tree construction algorithms.

Overall dimension 1 seems to outperform 0 and 2 for both Euclidean and cosine metric, and there is no clear winner between the two metrics. It is, however, surprising that Euclidean metric with 2-dimensional topological features is not too far behind. When we look at the persistence diagrams on Figure 9, we see that the 2-dimensional diagrams for Euclidean metric are somewhat sparse and all the features seem to be close to the diagonal. Indeed, probing all the diagrams, the maximum persistence of 2-dimensional features is roughly comparable to the smallest distance between the embeddings of any two words for the given language. Since features can pop up or disappear at the diagonal with small perturbations of data, such low-persistent features would often be discarded as noise. Yet, in combination with bars statistics distance, the trees constructed with UPGMA algorithm based on this data are among the best performing in our analysis.

From the persistence diagram distances, sliced Wasserstein and bars statistics lead to clearly stronger results than bottleneck distance and persistence images. Bottleneck distance is expected to be subpar, as having one more or one fewer feature can already yield a large distance. It is a bit less clear why persistent images do not perform so well, especially when they should approximate 1-Wasserstein distance just as the sliced Wasserstein. One possible reason is that the method has many parameters and our choice might not be ideal—we chose range, for both birth and death, $(0, 1)$, $\sigma = .1$, for cosine; and $(0, 10)$, $\sigma = 1$, for Euclidean; grid 10×10.

# σ from mean	j_k1	j_k2	mat	phy	clust	path	mean
Euclidean, dim 0	2.19	2.54	1.37	2.14	2.19	0.83	1.88
Euclidean, dim 1	**2.74**	**2.57**	2.33	2.74	3.10	1.14	2.43
Euclidean, dim 2	2.38	2.17	2.17	2.38	2.74	0.76	2.10
cosine, dim 0	2.19	2.19	1.53	2.63	2.58	0.62	1.95
cosine, dim 1	2.41	2.14	**2.58**	**3.28**	**3.27**	**1.46**	**2.52**
cosine, dim 2	1.72	1.36	1.76	2.89	2.71	0.93	1.90
bottleneck	1.80	1.70	1.57	2.28	2.36	0.93	1.78
sliced Wasserstein	**2.63**	**2.49**	**2.40**	2.95	3.12	**1.05**	**2.44**
persistence image	2.25	2.17	1.69	2.21	2.38	0.88	1.93
bars statistics	2.40	2.28	2.17	**3.26**	**3.19**	0.97	2.38
nj	2.20	2.14	1.70	2.48	2.65	0.90	2.01
upgma	**2.34**	**2.18**	**2.21**	**2.88**	**2.87**	**1.02**	**2.25**

Table 1: Averages of the values presented in Figure 2 (number of standard deviations away from the mean). In each block we fix one of the parameters, and aggregate over all others.

# $\geq$ 99500	j_k1	j_k2	mat	phy	clust	path	sum
Euclidean, dim 0	6	**6**	2	6	4	0	24
Euclidean, dim 1	**8**	4	4	7	12	0	35
Euclidean, dim 2	7	3	**8**	6	9	0	33
cosine, dim 0	2	1	2	5	7	0	17
cosine, dim 1	5	3	6	**13**	**14**	**1**	**42**
cosine, dim 2	2	0	4	10	10	0	26
bottleneck	4	2	3	9	12	0	30
sliced Wasserstein	10	**7**	9	14	**19**	0	59
persistence image	5	3	4	7	8	0	27
bars statistics	**11**	5	**10**	**17**	17	**1**	**61**
nj	12	7	8	15	21	0	63
upgma	**18**	**10**	**18**	**32**	**35**	**1**	**114**

Table 2: The number of dots in Figure 2 corresponding to parameters that performed better than 99,500 random permutations of the tree leaves (labeled by star in the figure). The total number of dots for a fixed distance that meet the parameters in each block is 24, 36 and 72, respectively.

full fig	all	jrf_k1	jrf_k2	match	phylo	clust	path
total	864	144	144	144	144	144	144
$\sigma > 1$	681	121	111	117	134	134	64
$\sigma > 2$	451	84	74	72	99	103	19
$\sigma > 3$	229	36	41	29	59	63	1
$\sigma > 4$	74	13	15	7	17	22	0
$\sigma > 5$	17	2	4	1	5	5	0
$\sigma > 6$	5	0	2	0	2	1	0
30 lang	all	jrf_k1	jrf_k2	match	phylo	clust	path
total	288	48	48	48	48	48	48
$\sigma > 1$	242	43	40	43	44	45	27
$\sigma > 2$	155	31	31	24	26	30	13
$\sigma > 3$	69	12	19	11	13	13	1
$\sigma > 4$	22	3	4	3	4	8	0
$\sigma > 5$	7	1	1	1	2	2	0
$\sigma > 6$	4	0	1	0	2	1	0
50 lang	all	jrf_k1	jrf_k2	match	phylo	clust	path
total	288	48	48	48	48	48	48
$\sigma > 1$	230	40	36	39	47	46	22
$\sigma > 2$	162	28	26	24	40	40	4
$\sigma > 3$	92	16	17	10	23	26	0
$\sigma > 4$	39	8	9	2	10	10	0
$\sigma > 5$	9	1	3	0	3	2	0
$\sigma > 6$	1	0	1	0	0	0	0
81 lang	all	jrf_k1	jrf_k2	match	phylo	clust	path
total	288	48	48	48	48	48	48
$\sigma > 1$	209	38	35	35	43	43	15
$\sigma > 2$	134	25	17	24	33	33	2
$\sigma > 3$	68	8	5	8	23	24	0
$\sigma > 4$	13	2	2	2	3	4	0
$\sigma > 5$	1	0	0	0	0	1	0
$\sigma > 6$	0	0	0	0	0	0	0

Table 3: The number of parameters in Figure 2 with value greater than a given threshold.

full fig	all	jrf_k1	jrf_k2	match	phylo	clust	path
total	864	144	144	144	144	144	144
top 10.00%	613	113	102	98	121	128	51
top 5.00%	484	90	75	76	102	112	29
top 1.00%	255	39	34	42	65	72	3
top 0.50%	177	30	17	26	47	56	1
top 0.10%	57	10	4	10	14	19	0
top 0.05%	32	5	3	5	9	10	0
top 0.01%	10	1	2	2	2	3	0
30 lang	all	jrf_k1	jrf_k2	match	phylo	clust	path
total	288	48	48	48	48	48	48
top 10.00%	217	40	39	33	36	44	25
top 5.00%	172	34	33	26	28	34	17
top 1.00%	75	13	15	14	12	18	3
top 0.50%	46	11	5	9	9	11	1
top 0.10%	16	2	1	3	4	6	0
top 0.05%	9	1	1	3	2	2	0
top 0.01%	5	1	1	1	1	1	0
50 lang	all	jrf_k1	jrf_k2	match	phylo	clust	path
total	288	48	48	48	48	48	48
top 10.00%	212	38	33	34	47	43	17
top 5.00%	169	30	25	25	41	41	7
top 1.00%	100	17	15	13	27	28	0
top 0.50%	74	13	10	9	18	24	0
top 0.10%	29	6	3	3	8	9	0
top 0.05%	18	3	2	1	6	6	0
top 0.01%	3	0	1	0	1	1	0
81 lang	all	jrf_k1	jrf_k2	match	phylo	clust	path
total	288	48	48	48	48	48	48
top 10.00%	184	35	30	31	38	41	9
top 5.00%	143	26	17	25	33	37	5
top 1.00%	80	9	4	15	26	26	0
top 0.50%	57	6	2	8	20	21	0
top 0.10%	12	2	0	4	2	4	0
top 0.05%	5	1	0	1	1	2	0
top 0.01%	2	0	0	1	0	1	0

Table 4: The number of parameters in Figure 2 with distance smaller than the given percentage of the 100,000 permutations.

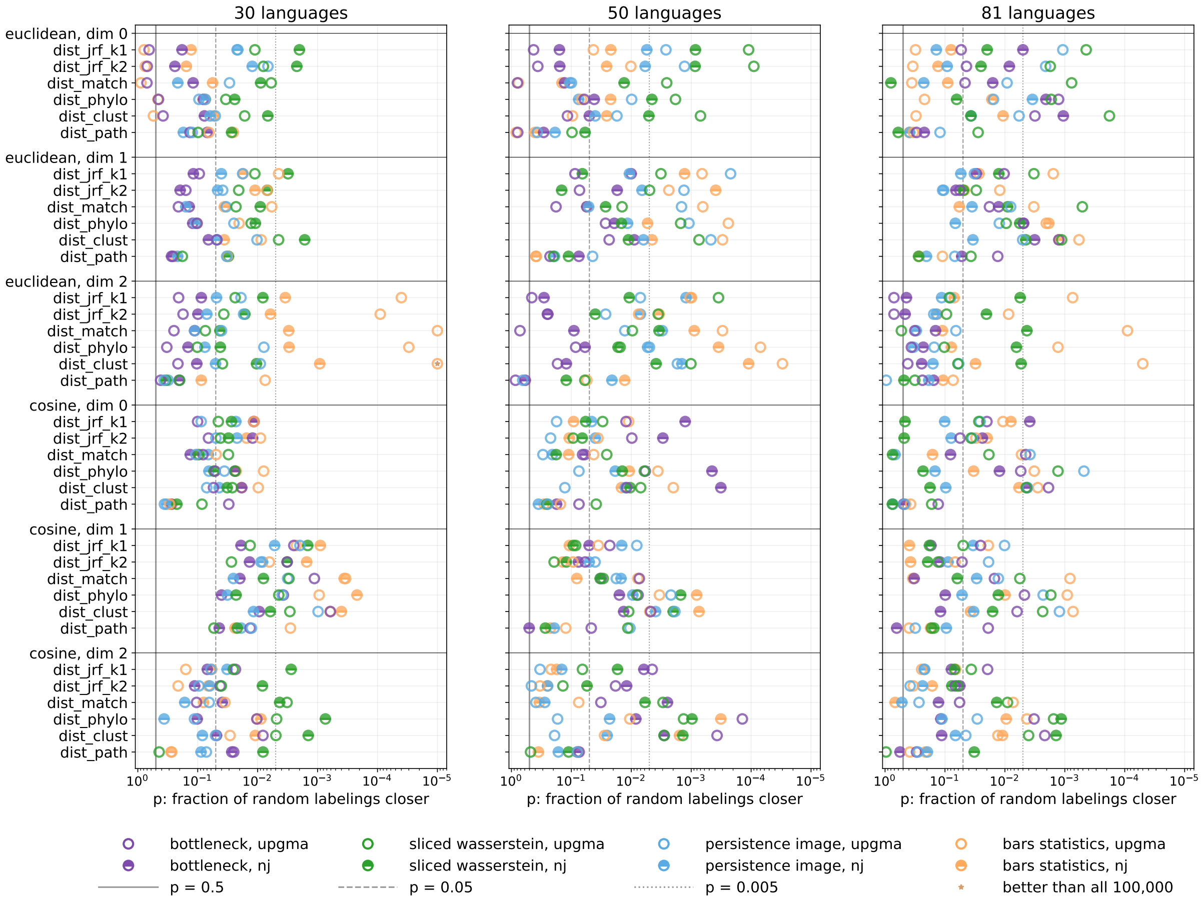

Figure 6: The statistical significance of TDA trees for 30, 50, and 81 languages against the Ethnologue reference for trees reconstructed by UPGMA and NJ for each combination of parameters described in Section 4, as in Figure 2. Each dot represents the distance of a single reconstructed tree to the reference, and its position shows what fraction of 100,000 random permutations of the tree's leaves lead to smaller distances.

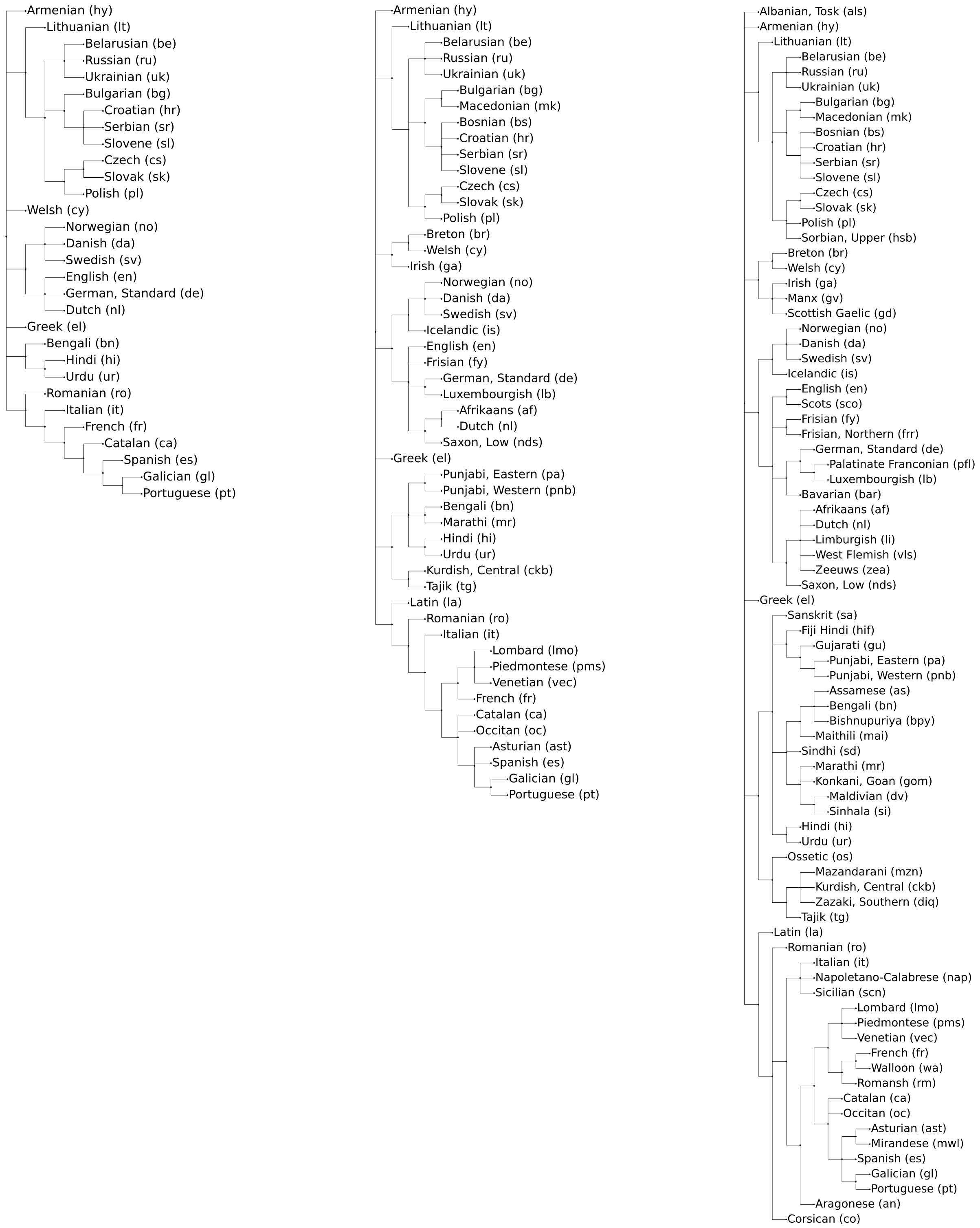

Figure 7: The reference Ethnologue language phylogenic trees (Lewis et al., 2024) employed in this study, for sets of the most popular 30, 50 and 81 Indo-European languages with FastText word embeddings.

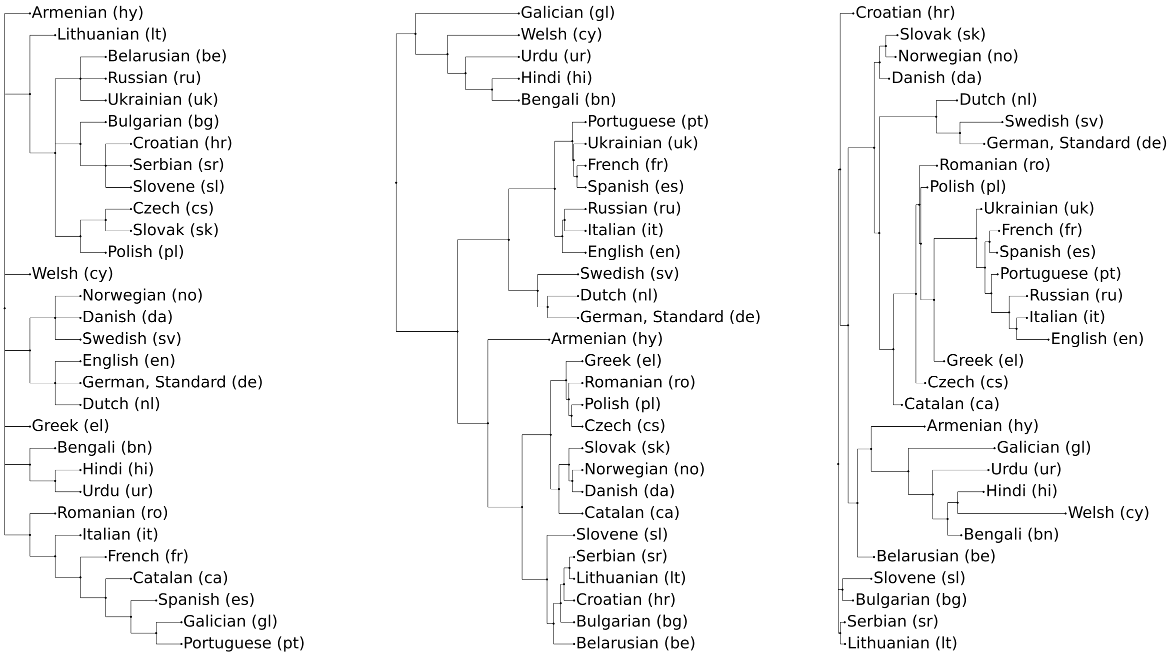

(a) Reference Ethnologue tree

(b) UPGMA

(c) NJ

Figure 8: The 30-language reference Ethnologue tree with representative UPGMA and NJ reconstructed trees using TDA (here 2-dimensional persistent homology using Euclidean distance and inferred distances between languages based on bars statistics between the persistent diagrams). Although far from perfect agreement, the reconstructed trees captures many meaningful language subgroups; for UPGMA, e.g. (i) clusters of Balto-Slavic languages (*sl*, *sr*, *lt*, *hr*, *bg*, *be*), (ii) the Romance Italo-Western group (*pt*, *fr*, *es*, *it*) mixed with Germanic languages (*de*, *nl*, *en*, *sv*), while (iii) the more distant Indo-Aryan languages (*bn*, *hi*, *ur*) are clustered and well-separated.

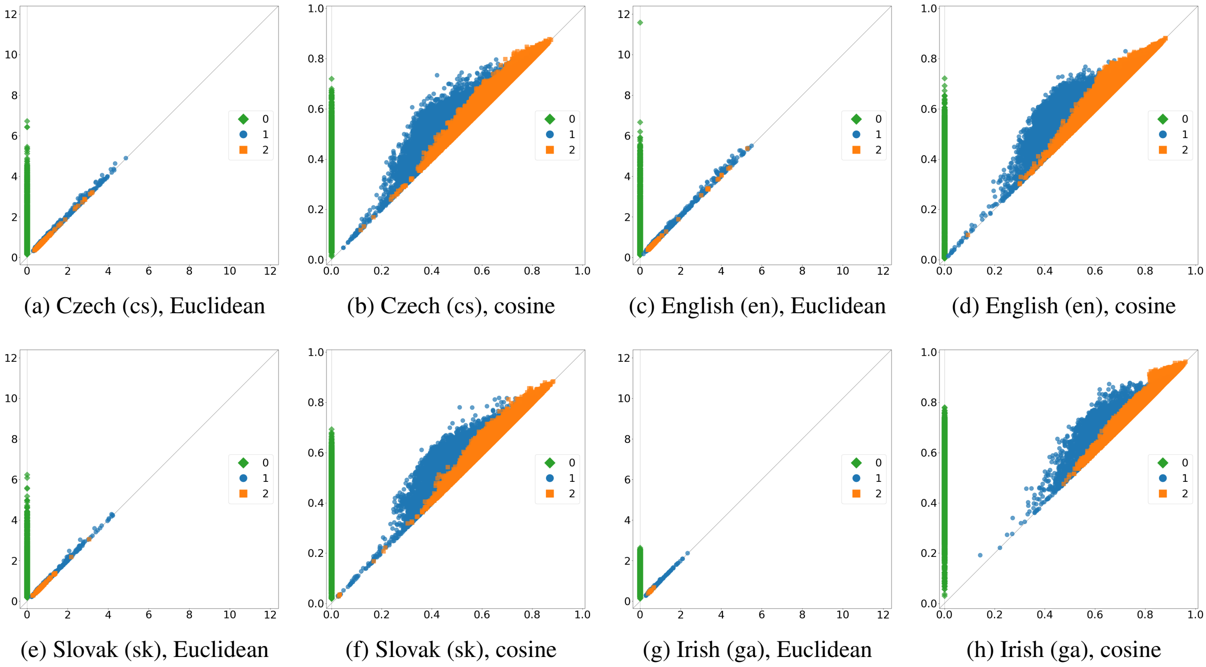

(a) Czech (cs), Euclidean

(b) Czech (cs), cosine

(c) English (en), Euclidean

(d) English (en), cosine

(e) Slovak (sk), Euclidean

(f) Slovak (sk), cosine

(g) Irish (ga), Euclidean

(h) Irish (ga), cosine

Figure 9: Eight persistence diagrams for language embeddings analysed in this paper including Czech and Slovak, which are very closely related, and English and Irish, which belong to distant branches (Germanic and Celtic) of the Indo-European family. For each language we show diagrams for distinct Euclidean and cosine metrics. Each diagram shows features for dimensions 0, 1 and 2, that is, connected components, loops, and 2-spheres.